

**THE UNIVERSITY OF WESTERN ONTARIO
DEPARTMENT OF CIVIL AND
ENVIRONMENTAL ENGINEERING**

Water Resources Research Report

**Modelling of High Resolution Flow from GCM
Simulated Runoff using a Mesoscale
Hydrodynamic Model: CAMA-FLOOD**

**By:
Ayushi Gaur
Abhishek Gaur
and
Slobodan P. Simonovic**

**Report No: 101
Date: October 2017**

**ISSN: (print) 1913-3200; (online) 1913-3219
ISBN: (print) 978-0-7714-3154-8; (online) 978-0-7714-3155-5**



MODELLING OF HIGH RESOLUTION FLOW FROM GCM SIMULATED RUNOFF
USING A MESOSCALE HYDRODYNAMIC MODEL: CAMA-FLOOD

By

Ayushi Gaur

Abhishek Gaur

and

Slobodan P. Simonovic



Department of Civil and Environmental Engineering

Western University, Canada

October 2017

Executive Summary

Large scale modelling of river hydrodynamics is essential for understanding processes within the hydrologic cycle. It is also useful in many other interdisciplinary research fields like earth system modelling, flood risk assessment etc.

Catchment-based Macro-scale Floodplain model (CaMa-Flood) is a recently developed mesoscale hydrodynamic model that has been used to perform continental and global scale flow simulations. In the model, study area is divided into grids of user-defined spatial scale. Upstream area contributing to the outflow from each grid, referred as a “unit catchment” is calculated for each grid. Gridded flow direction map is obtained using a novel FLOW method which facilitates accurate delineation of water flow between grids. Water balance calculations are performed at each grid cell and generated flow is routed along the flow direction map. Water storage is the only prognostic variable in the model while other variables such as water-level, flooded area etc. are estimated empirically. CaMa-Flood has been tested for computational efficiency and has been found to be significantly more efficient than other state-of-the-art mesoscale hydrodynamic models that are used today. In this report, the structure of CaMa-Flood has been explained, followed by a detailed procedure of obtaining higher resolution gridded flow output across Canada from low-resolution global GCM runoff simulations has been presented. The implementation has been performed on Shared Hierarchical Academic Research Computing Network (SHARCNET) platform to be able to complete simulations within a manageable time-frame.

Table of Contents

1.	Introduction	5
2.	Catchment based Macro-scale Floodplain Model (CaMa-Flood)	11
2.1.	Model structure	11
2.2.	Delineation of high resolution flow direction map	13
2.3.	Hydrodynamic calculations	15
3.	Methodology	18
3.1.	Extraction of runoff data from the GCMs	18
3.2.	Preparation of input files for CaMa-Flood	18
3.3.	Running CaMa-Flood on SHARCNET	19
3.4.	Processing generated outputs	23
4.	Sample simulation.....	24
5.	Summary	31
6.	References	33
7.	Appendix A	37
8.	Appendix B: List of Previous Reports in the Series	39

List of Tables

Table 3.1.	List of directories in the CaMa-Flood package	21
------------	---	----

List of Figures

Figure 2.1.	River channel reservoir and floodplain reservoir defined in each grid point of CaMa-Flood.....	11
Figure 2.2.	Unit-catchments delineated from a high-resolution flow direction map	12
Figure 2.3.	Procedure for obtaining flow direction map	14
Figure 3.1.	WinSCP login window	20
Figure 3.2.	PuTTY configuration window	20
Figure 3.3.	Commands to set the modules and paths in Mkinclude file	22
Figure 3.4.	Code to submit the jobs in PuTTY and run the code on SHARCNET	23
Figure 3.5.	List of output variables from CaMa-Flood	23
Figure 4.1.	Locating grids of CaMa-Flood inputs coordinates lying within Canada	25
Figure 4.2.	Sample input runoff files for CaMa-Flood for the GCM for historical and future for each day	26
Figure 4.3.	Editing in global_15min.sh file for getting the desirable timeline and output variables	26
Figure 4.4.	Edited Mkinclude file for CaMa-Flood model simulation	27
Figure 4.5.	Transferring input files to the CaMa-Flood package input folder	28
Figure 4.6.	Code compilation and creating executables	28
Figure 4.7.	Final code for running CaMa-Flood model simulation in PuTTY software	29
Figure 4.8.	Output flood area files generated from CaMa-Flood	30

1. Introduction

Climate change is expected to bring considerable changes in hydro-climatic regimes across the globe. Changes have already been recorded and several studies have investigated changes in future climatic conditions and flow dynamics. In recent decades capabilities of runoff modeling at continental and global scale have increased exponentially owing to an increase in computational resources and the availability of remotely sensed geophysical datasets. Past studies that have analyzed future changes in flow and flow extremes have been briefly reviewed here.

Dankers and Feyen (2008) estimated future flood hazard for Europe. Future climatic projections at 12 km resolution from two regional climate models (RCMs): HIRHAM model of the Danish Meteorological Institute (Larsen et al., 2014) and the Rossby Centre Atmosphere Ocean Model (RCAO) of the Swedish Meteorological and Hydrological Institute (Environment Climate Data Sweden, 2017). They were used as inputs into a hydrological model: LISFLOOD to simulate future river discharges across Europe for historical (1961-1990) and future (2071-2100) timelines. LISFLOOD hydrologic model is a combination of gridded water balance model and a one dimensional hydrodynamic channel flow routing model (Dankers et al., 2008). Future climatic projections corresponding to SRES greenhouse gas emission scenarios A2 and B2 were considered (IPCC, 2000; Nakicenovic et al., 2000). Flood frequency analysis was performed by fitting a Generalized Extreme Value (GEV) distribution to annual maximum flows. It was found that by the end of this century under A2 emission scenario, extreme discharges in many European rivers are likely to increase in magnitude and frequency. It was also estimated that the recurrence interval of the present day 100-year flood event might decrease to 50 years or less in many parts of Europe.

Lehner et al. (2006) simulated changes in the frequency and magnitude of future floods and droughts in Europe. Analysis was performed on 100-year return period flood and drought events. A global integrated water model Water- Global Assessment Prognosis (WaterGAP) was used to simulate flows. The Global Hydrology Model, that is a part of the WaterGAP model, calculates runoff at each grid cell by performing water balance and water routing calculations along the global drainage direction map (Doll and Lehner, 2002). Future flow projections were made by using climatic projections simulated by two state-of-the-art global climate models (GCMs) ECHAM4 (Stevens et al., 2012) and HadCM3 (Gordon et al., 2000) following future greenhouse gas emission scenario A1B. Results indicated an increase in the frequency of floods in northern to northeastern Europe and increase in drought frequency for southern to southeastern Europe.

Arnell (1999) assessed the implications of climate change on global water resources. This work used two global climate models from Hadley Centre Climate Simulations (HadCM2 and HadCM3) (Gregory et al., 2000) to perform water balance calculations at $0.5^\circ \times 0.5^\circ$ spatial scale. Future flows were projected using a macro-scale hydrodynamic model by using climate variables as input into the model. Each individual GCM grid was considered separate from each other and projected future changes in water storage were analyzed at each GCM grid-cell. Results indicated that runoff projections obtained from both models were found similar but important regional differences were obtained from both the GCMs. Future projections of changes in water stress across the country have been analyzed using both GCMs for two different timelines. In case of HadCM2 scenario, population in countries with water stress would increase by 53 million by the end of 2025. However, under HadCM3 scenario the population in countries with water stress would rise by 113 million for the same time-period. By the end of 2050, there would be a net reduction in population stressed countries under HadCM2 (~69 million) but an increase of 56 million under HadCM3.

Gosling and Arnell (2013) used future climatic projections made by 21 GCMs under SRES scenarios B1, B2, A1B, and A2 as inputs into a global scale hydrologic model, Mac-PDM.09 (Gosling et al., 2010) to simulate current and future flow regimes at 0.5°x0.5° spatial resolution. Water scarcity was calculated using a global water resources model (Arnell et al. 2011; Gosling et al. 2010). Results indicated increase in exposure to water scarcity for most of the world and projected to vary for different future climate scenarios due to the increase of global mean temperature.

Doll and Schmied (2012) used future climate projections made by the ECHAM4 GCM (Steven et al., 2012) and simulated future changes in flow regimes across the globe using a global hydrologic model WaterGAP (Alcamo et al., 2010). In WaterGAP hydrologic model runoff calculated from the vertical water balance is routed laterally within the grid through groundwater and “local” surface water storages. Further runoff is also routed downstream to several “global” surface water storages.

Doll and Zhang (2010) quantified climate change impact on future flows at a global scale using WaterGAP model. Future climatic projections made by two global climate models ECHAM4 and HadCM3 under two future emission scenarios A2 and B2 were used to generate future flows. Results indicated that flow magnitude and timing is expected to change considerably at approximately 90% of the global land area.

Veijalainen et al (2010) performed a continental scale study over Finland where future changes in flooding due to climate change were analyzed for two time slices 2010-2039 and 2070-2099. Changes in flooding were estimated at 67 catchments with variable sizes. A total of 20 future climatic projections corresponding to 3 future emission scenarios were used to simulate future

flows. The hydrological simulations were performed using Watershed Simulation and Forecasting System (WSFS) (Vehviläinen and Bertel, 1994). Flood frequency analysis was performed for 100-year return period flooding event by fitting annual maximum flows to Gumbel distribution. The inundation areas of the 100-year floods were estimated using a 2-D hydraulic model. Results indicated that the impact of climate change is not uniform across the watersheds due to regional climate variability and watershed properties. In case of snowmelt flood dominating areas, frequency of annual floods will decrease or remain unchanged due to decreasing snow accumulation.

Changes in peak river flows across Britain between two time slices, 1960-1990 and 2069-2099 were estimated by Bell et al. (2016). Climatic projections from two Regional Climate Models are used as inputs into the G2G (Grid-to-grid) distributed hydrological model (Bell et al., 2009). Results indicated high spatial variability in the projected percent changes in peak flow magnitudes and large uncertainty in projected changes. Changes in projected future peak flows were also compared to an estimate of current natural variability, where most of the changes were found to fall outside the range of natural variability in southern Britain.

Arheimer et al. (2015) performed a climate change impact assessment on flooding frequency and magnitudes in the past and the future (1911-2100) over 69 gauging stations across Sweden. Future climate variable projections from two global climate models HadCM3Q0 (Johns et al. 2003; Collins et al. 2006) and ECHAM5r3 (Roeckner et al. 2006) were used as inputs into SHYPE hydrologic model to generate flows. Results indicated projected earlier spring floods in the northern-central part of Sweden. High-flows are projected to become more frequent in the southern part of the Sweden.

Sorribas et al. (2016) determined climate change effects on river discharge and flood inundation extent for the Amazon basin between present and one future timeline, 2070-2099. Future climate projections from 5 GCMs for RCP8.5 scenario were used for analysis. A large-scale regional hydrological model MGB-IPH (Collischonn et al., 2010), which has a 1-D regional river hydraulic model was used to perform water storage simulations on floodplains. Results projected changes in flows and flood inundation extent across Amazon basin. Hydro-climatic projections were found to be associated with considerable uncertainty. Results indicated increased mean river discharge and flood extent in western Amazonia. Decreased river discharges were projected for eastern basins of Amazonia and decreased inundation extent in the central and lower Amazon.

Yamazaki et al. (2012) used runoff simulations as inputs made by a Land Surface Scheme within the GCMs across the Amazon River basin and simulated high-resolution water level dynamics using a macro-scale hydrodynamic model: Catchment-based Macro-scale Floodplain Model (CaMa-Flood). A comparison of CaMa-Flood simulated water level dynamics with the observations showed that CaMa-Flood is able to accurately simulate water level dynamics for a large scale catchment like the Amazon. This approach was innovative in the sense that water balance and energy budget calculations were performed within the GCMs at low spatial resolution (1° to 3° spatial scale) while routing was performed at much higher resolution (25 km spatial scale). Further, sub-grid parameters like slope, river length, channel width, channel depth were considered while routing flow at each grid within the CaMa-Flood model. Sub-grid parameters were estimated by using an innovative upscaling method FLOW.

Hirabayshi et al. (2013) performed a global scale flow and flood risk change assessment study using runoff projections from 11 (out of 23) GCMs. Gridded runoff projections from the GCMs used were used as input into a macro-scale hydrodynamic model CaMa-Flood, and high resolution

gridded runoff was produced and routed downstream using a river network map. Calculation of river discharge was performed for the time period 1960-2100. Changes in flood magnitude and frequency between present and the end of 21st century time-periods were analyzed. Results indicated large increase in flood frequency in Southeast Asia, Peninsular India, eastern Africa and the northern half of the Andes. However, some parts of the world were also projecting decrease in flood frequency.

Rest of the report is organized as follows. Chapter 2 presents a theoretical framework of the macroscale hydrodynamic model for generating high-resolution flow is described in this section. Chapter 3 presents the methodology that has been adopted for high resolution runoff simulation using macroscale hydrodynamic model CaMa-Flood; preparation of runoff inputs for CaMa-Flood using R programming language; use of SHARCNET (Shared Hierarchical Academic Network) for high speed runoff simulation by CaMa-Flood. Chapter 4 presents the summary made by this report.

2. Catchment based Macro-scale Floodplain (CaMa-Flood) Model

2.1 Model structure

CaMa-Flood is distributed global river routing model that can be used to simulate water level dynamics at regional to global scales. It routes the high-resolution flow from one grid cell to another along a prescribed river network map. Each grid point has a river channel reservoir and floodplain reservoir, (Figure 2.1).

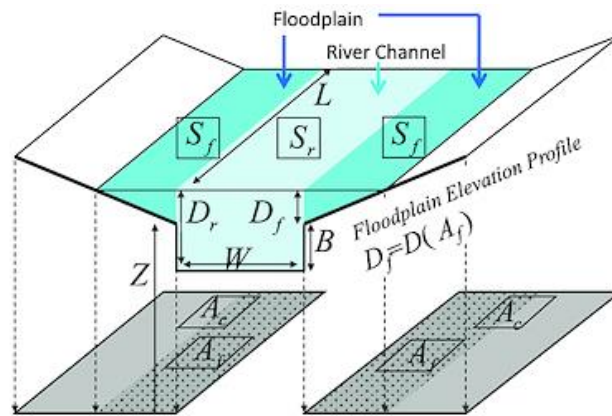


Figure 2.1. River channel reservoir and floodplain reservoir defined in each grid point of CaMa-Flood (Yamazaki et al, 2011).

Water storage is the only prognostic output from the CaMa-Flood for each grid. Other variables like river discharge, water surface elevation, flooded area, total outflow; water depth etc. are derived empirically from water storage. The parameters and variables used in the CaMa-Flood are: channel length (L), channel width (W), and bank height (B). A floodplain reservoir has a parameter for unit catchment area, A_c , and a floodplain elevation profile, $D_f = D(A_f)$, which describes

floodplain water depth, D_f , as a function of flooded area, A_f . The assumption made in the model is that inundation will always occur from lower to higher resolution.

Each grid point has a river channel and a floodplain reservoir as shown in the Figure 2.2. CaMa-Flood performs all the computation on unit-catchment scale. A unit-catchment area for each grid is the area that contributes to the runoff from each grid and collects at the outlet of the grid. In order to achieve efficient flow computation at global scale, the entire river networks of the world are discretized unit-catchments, see Figure 2.2.

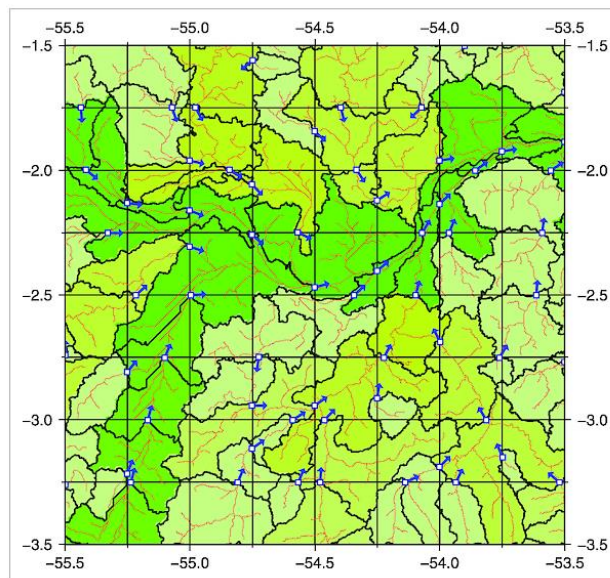


Figure 2.2. Unit-catchments delineated from a high-resolution flow direction map. Red lines are the streams derived from flow direction map. One outlet pixel is assigned to each 0.25 degree grid box. Areas divided by black boundaries indicate the unit-catchment of each grid point (Yamazaki et al, 2011). The blue vector of each outlet pixels indicates the downstream direction.

2.2 Delineation of high resolution flow direction map

In Flexible Location of Waterways (FLOW) method, the downstream grid cell of the upscaled river network map can be located away from the immediate neighborhood of the cell as opposed to previous methods where downstream cell was always considered as one of the eight neighboring cells. Two datasets are required to prepare flow direction map using FLOW method: (1) surface elevation map, and (2) river network map. Following steps are preformed (refer to Figure 2.3).

- From among the pixels located on the border of a target cell, pixel with largest upstream area is marked as potential outlet pixel for that cell.
- The flow path is traced from the fine resolution flow direction map until it reaches another outlet pixel downstream.
- Pixels lying between upstream and downstream potential outlet pixels are known as river channel pixels of the target cell.
- The river channel length is calculated along the fine resolution flow direction map.
- The pixels between two potential outlet pixels are defines as the “river channel pixels” of the target cells. The river channel length of a target cell is measured along the fine-resolution flow path, with the diagonal step distance taken to be $\sqrt{2}$ times of the pixel size, know as the threshold value of channel length.
- If measured river channel length is shorter than the threshold value of channel length (as discussed in the previous step), again new outlet pixel is selected from the remaining.

- outlet pixels and above steps are repeated until the river channel length becomes longer than the threshold value and thus the final outlet pixels are accepted.

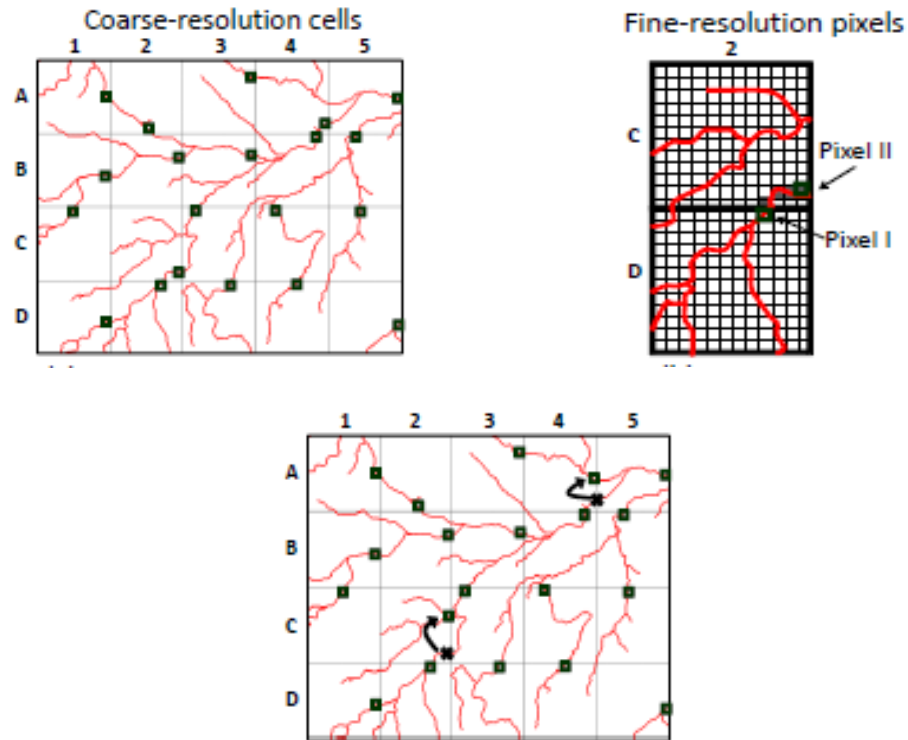


Figure 2.3. Procedure for obtaining flow direction map. Outflow pixels at each cell are obtained first which are connected along the river network map to obtain final flow direction map (Yamazaki et al., 2009).

2.3 Hydrodynamic calculations

2.3.1 Water level

Water level is calculated from the water storage at each grid cell. River channel water storage, S_r , floodplain water storage, S_f , river water depth, D_r , floodplain water depth, D_f , and flooded area,

A_f , are obtained from the total water storage of a grid point, S . Water level is calculated by comparing the total water storage, S of a grid cell with the flood initiation storage, S_{ini} , $S_{ini}=BWL$, where B is channel depth, W is channel width, and L is channel length. When S is less or equal to S_{ini} , following equations are applied to calculate water level:

$$S_r = S \quad \dots (1)$$

$$D_r = S_r / WL \quad \dots (2)$$

$$S_f = 0 \quad \dots (3)$$

$$D_f = 0 \quad \dots (4)$$

$$A_f = 0 \quad \dots (5)$$

For the case that the total water storage, S , is greater than the flood initiation storage, S_{ini} , the simultaneous equations are applied:

$$S_r = S - S_f \quad \dots (6)$$

$$D_r = S_r / WL \quad \dots (7)$$

$$S_f = \int_0^{A_f} (D_f - D(A)) dA \quad \dots (8)$$

$$D_f = D_r - B \quad \dots (9)$$

$$A_f = 0 \quad \dots (10)$$

The Equation (9) means that the water surface elevations of the river channel and the floodplain are same. This equation is based on the assumption that water mass is instantaneously exchanged between the channel and the floodplain to balance the water surface elevations of the two reservoirs.

2.3.2. River discharge

The river discharge from each cell toward its downstream cell is calculated using the river network map. The river discharge is calculated with the local inertial equation (Bates et al., 2010). The local inertial equation is derived by neglecting the second term of the St. Venant momentum equation:

$$\frac{\partial Q}{\partial t} + \frac{\partial}{\partial x} \left[\frac{Q^2}{A} \right] + \frac{gA\partial(h+z)}{\partial x} + \frac{gn^2Q^2}{R^{4/3}A} = 0 \quad \dots (11)$$

where Q is the river discharge (m^3s^{-1}), A is the flow cross section area (m^2), h is the flow depth (m), z is the bed elevation (m), R is the hydraulic radius (m), g is the acceleration due to gravity (ms^{-2}), and n is the Manning's friction coefficient ($\text{m}^{-1/3}\text{s}^{-1}$). The x and t are the flow distance and time, respectively. The first, second, third and fourth terms represent the local acceleration, advection, water slope, and friction slope, respectively. The explicit form of the local inertial equation (12) is used in the CaMa-Flood model.

$$Q^{t+\Delta} = \frac{Q^t - \Delta t g A S}{\left(1 + \frac{\Delta t g n^2 |Q^t|}{R^{4/3} A}\right)} \quad \dots (12)$$

where S is the water surface slope. Q^t is the discharge at the previous time step, and $Q^{t+\Delta t}$ is the river discharge between the time t and $t+\Delta t$. The hydraulic radius R is approximated by flow depth h_{flw} . The Manning's coefficient is set to $n=0.03$.

The negative river discharge, which may occur in the calculation by the local inertial equation and the diffusive wave equation, represents the backward water flow from the downstream grid cell towards the current grid cell.

2.3.3 Storage change

The storage change at each grid cell from the time t to $t+\Delta t$ is calculated by the mass conservation equation:

$$S_i^{t+\Delta t} = S_i^t + \sum_k^{Upstream} Q_k^t \Delta t - Q_i^t \Delta t + A c_i R_i^t \Delta t \quad \dots (13)$$

where S_i^t and $S_i^{t+\Delta t}$ represent the water storage of grid i at the time t and $t+\Delta t$, Q_i^t represents the river discharge outflow from grid i at time t , Q_k^t represents the river discharge inflow from the upstream grid k , $A c_i$ is the unit catchment area of grid i , and R_i^t represents the input runoff to the grid i .

2.3.4 Calculation of floodplain flow

Floodplain discharge is also calculated by the local inertial equation (12). The flow area A is calculated by dividing floodplain storage by channel length. The flow depth h is given by the floodplain depth. The Manning's coefficient for floodplain flow is set to $n=0.10$.

3. Methodology

Methodology for generating high-resolution flow by CaMa-Flood simulations is provided in this Chapter and subdivided into four sections: (i) extraction of runoff data from the GCMs, (ii) preparation of input files for SHARCNET computation, (iii) running CaMa-Flood on the SHARCNET, and (iv) processing generated outputs.

3.1 Extraction of runoff data from the GCMs

Runoff datasets are obtained in NetCDF (*.nc) file format and are accessed and analyzed using R statistical and programming language (R Development Core Team, 2008). The data can be extracted for all grids located within the desired location.. Extracted data are saved as numeric.

3.2 Preparation of input files for CaMa-Flood

Extracted runoff datasets are first interpolated at $1^{\circ} \times 1^{\circ}$ spatial resolution on grids arranged from 180W to 180E and from 90N to 90S as input data in the CaMa-Flood model used in this study should be arranged in that order. Interpolation is performed using Inverse Distance Squared method. According to this method, data at a particular location is inversely proportional to the square of distance from the nearest model grid point. The distance of point of interpolation is found out from four nearest reanalysis data grid points surrounding it. ECMWF periodically uses its forecast models and data assimilation systems to 'reanalyse' archived observations, creating global data sets describing the recent history of the atmosphere, land surface, and oceans. Reanalysis data allows for a close monitoring of the Earth's climate system also where direct observations are

sparse. It is mostly used for monitoring climate change, for research and education, and for commercial applications. A simple formula, shown in Equation (14) is then used to calculate weight associated with each grid point. Interpolated value at a particular location (v_i) is calculated by finding the sum of weighted means of climate data at all four grid points (v_j) using Equation (15).

$$w_j = \frac{1/d_j^2}{1/d_1^2 + 1/d_2^2 + 1/d_3^2 + 1/d_4^2} \quad \dots 14$$

$$v_i(t) = \sum_{j=1}^4 w_j * v_j(t) \quad \dots 15$$

where d_1 , d_2 , d_3 and d_4 are the distances of the location of interpolation from four nearest grid points and w_j is the weight calculated for j^{th} grid point. The data is also converted from numeric format to binary format. The byte order is “little endian”.

3.3 Running CaMa-Flood on the SHARCNET

CaMa-Flood is run on the SHARCNET to reduce computational time required to perform simulations. Following steps are performed to do so:

- Download and install WinSCP and PuTTY.exe (Figure 3.1, 3.2) software packages.

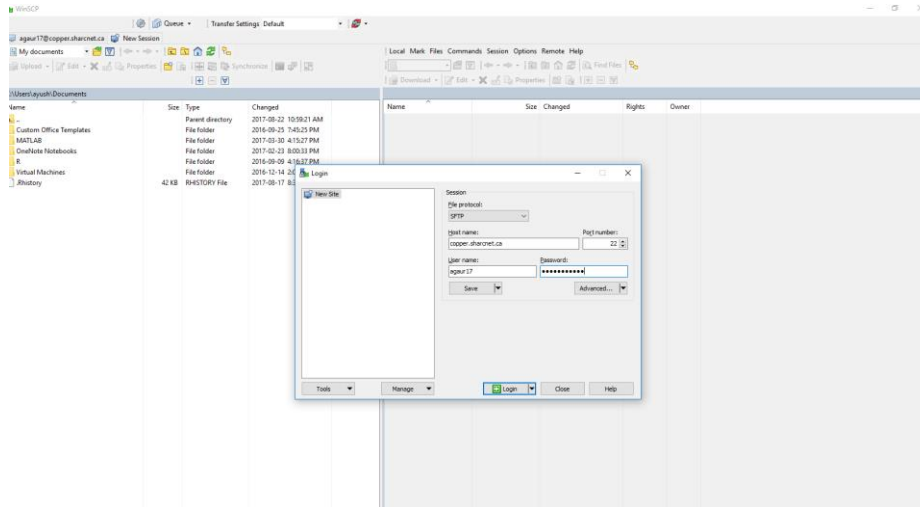


Figure 3.1. WinSCP window login window.

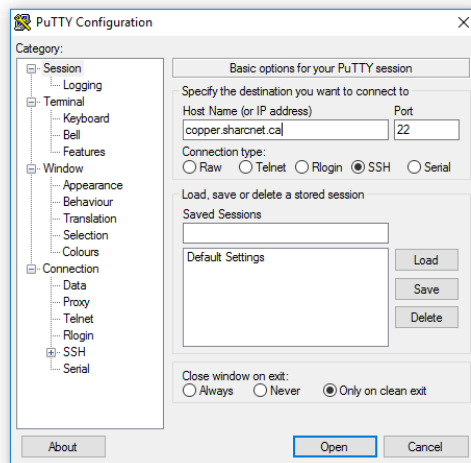


Figure 3.2. PuTTY configuration session window.

- Set the modules and paths first by running the commands shown in Figure 3.3. By doing so, SHARCNET will be able to find “gcc” and “ifort” compiler automatically. You need to set the modules and paths every time you login to SHARCNET.
- The directories present under the main directory \$CaMa-Flood/, are listed in Table 3.1.

Table 3.1. List of directories in the CaMa-Flood package.

Directories	Purpose
\$ (CaMa-Flood)/	Main Directory
adm/	Administration Directory, contains Mkinclude
gosh/	Shell Scripts Directory, for executing simulations
src/	Main Source Code Directory
lib/	Library Code Directory
mod/	Module Code Directory
map/	Map Directory, contains river network maps
inp/	Input Directory, contains a sample input data
out/	Output Directory, contains some programs for data processing
etc/	Various programs for analysis, visualization, etc.

- Modify the Mkinclude file to (as per the code shown in the Figure 3.3).

```

module unload intel mkl_ompmpi
module load intel/15.0.6

export LD_LIBRARY_PATH=/opt/sharcnet/testing/netcdf/4.3.2/lib:/opt/sharcnet/netcdf/4.3.2/lib:$LD_LIBRARY_PATH

RM = /bin/rm -f
CP = /bin/cp

# DMPI: activate when using MPI
# DCDF: activate when using netCDF
# DEND: activate when endian conversion is needed

#DMPI=-DUseMPI
#DCDF=-DUseCDF
#DEND=-DConvEnd
CFLAGS=${DMPI} ${DCDF} ${DEND}

### gfortran ###
INC = -I/opt/sharcnet/netcdf/4.3.2/include -I/opt/sharcnet/testing/netcdf/4.3.2/include
LIB = -L/opt/sharcnet/netcdf/4.3.2/lib -L/opt/sharcnet/testing/netcdf/4.3.2/lib -lnetcdf
#-lnetcdf

CPP = gcc -E $(CFLAGS)
FC = ifort -openmp

LFLAGS =
FFLAGS = -O3 -warn all -assume byterecl -heap-arrays
#FFLAGS = -O3 -Wall -g -fpe-trap=invalid,zero,overflow,underflow -fbounds-check -mcmode=medium -fbacktrace -fdump-core

### ifort ###
#INC = -I/usr/local/include
#LIB = -L/usr/local/lib -lnetcdf

#CPP = /usr/bin/gcc -E $(CFLAGS)
#FC = ifort -openmp
#FC = ifort

#LFLAGS =
#FFLAGS = -O3 -warn all -assume byterecl -heap-arrays

#FFLAGS = -O3 -Wall -g -fpe-trap=invalid,zero,overflow,underflow -fbounds-check -mcmode=medium -fbacktrace -fdump-core

### ifort ###
#INC = -I/usr/local/include
#LIB = -L/usr/local/lib -lnetcdf

#CPP = /usr/bin/gcc -E $(CFLAGS)
#FC = ifort -openmp
#FC = ifort

#LFLAGS =
#FFLAGS = -O3 -warn all -assume byterecl -heap-arrays

### MPI ###
#INC = -I/opt/local/include
#LIB = -L/opt/local/lib -lnetcdf
#FC = mpi90
#CPP = /usr/local/bin/gcc -E $(CFLAGS)
#LFLAGS =
#FFLAGS = -O3 -Wall

```

Figure 3.3. Commands to set the modules and paths in Mkinclude file.

- CaMa-Flood can take the advantage of multiple cores available on a particular node on SHARCNET. Following is the code to submit the jobs and run the code for instance on a node on a server (Copper in this case) which has 24 cores:

```
sqs sub -q threaded -n 24 -r 4h --mpp=16g -o outputfile.txt bash global_15min.sh
```

Figure 3.4. Code to submit the jobs in PuTTY and run the code on SHARCNET.

3.4 Processing generated outputs

Under default settings, CaMa-Flood generates 11 output variables listed in Figure 3.4. However, user defined outputs can also be obtained. The output files are obtained in plain binary format for the entire globe. Therefore, they need to be converted to numeric format as well as extracted over the region of interest.

File	Variable	Symbol	Description	Unit	Format
rivoutYYYYY.bin	rivout	Qr	River Discharge	[m3/s]	real
rivstoYYYYY.bin	rivsto	Sr	River Wter Storage	[m3]	real
rivdphYYYYY.bin	rivdph	Dr	River Water Depth	[m]	real
rivvelYYYYY.bin	rivvel	V	River Flow Velocity	[m/s]	real
fldoutYYYYY.bin	flddph	Qf	Floodplain Flow	[m3/s]	real
fldstoYYYYY.bin	fldsto	Sf	Floodplain Water Storage	[m3]	real
flddphYYYYY.bin	flddph	Df	Floodplain Water Deoth	[m]	real
fldareYYYYY.bin	fldare	Af	Flood Area	[m2]	real
fldfrcYYYYY.bin	fldfrc	Ff	Flood Fraction	[m2/m2]	real
sfcelvYYYYY.bin	sfcelv	WSE	Water Surface Elevation	[m]	real
outflwYYYYY.bin	outflw	Qall	Total Discharge (Qr + Qf)	[m3/s]	real
storgeYYYYY.bin	storge	Sall	Total Storage (Sr + Sf)	[m3]	real
pthoutYYYYY.bin	pthout	Qp	Net bifurcation flow from grid (ix,iy)	[m3/s]	real
pthflwYYYYY.pth	pthflw	-	Flow of bifurcation channel (ipth, ilev)	[m3/s]	real

Figure 3.5. List of output variables from CaMa-Flood.

4 Sample simulation

In this section, a more detailed account of the process involved to obtain higher resolution flow from low resolution runoff projections made by a representative GCM BCC-CSM-1-1 (Beijing Climate Center Climate System Model) is provided. Projections of carbon emission scenarios (RCP 2.6, RCP 4.5, RCP 6.0, RCP 8.5) as well as historical timelines for the duration 2061-2100 and 1961-2005 respectively are considered. Functions used for the preparation of input binary runoff data using R statistical and programming language is provided in Appendix A.

Steps used for the preparation of binary runoff inputs for CaMa-Flood simulation using R programming language is listed below:

4.1 Reading GCM runoff data using R programming language

The netCDF data file format from Unidata is a platform-independent, binary file that also contains metadata describing the contents and format of the data in the file. Version 4 of the netcdf library stores data in HDF5 format files; earlier versions stored data in a custom format. The R package `ncdf4` can read either format. NetCDF files also contain dimensions, which describe the extent of the variables arrays. Files not only contain the "data" but also a description of the variables, the creation history, and any other important attributes of the data set (Pierce. D., 2017). Runoff files in netCDF file format are accessed in R using the function provided in Appendix A (i). Runoff files are used to extract longitude, latitude information and time indices are extracted from the `ncfile`, and interpolation is performed to read the (.nc) runoff files. Some additional packages like `ncdf4`, `lubridate`, `ggplot2`, `reshape2` along with `ncdf4`, are used for performing various tasks. For

example, ncd4 is used to access .nc GCM files, lubridate is used for dates related functions, ggplot2 and reshape2 for plotting purposes, etc.

4.2 Extracting runoff projections for coordinates at which input data needs to be in CaMa-Flood.

In figure below (Figure 4.1), a data-frame “grids.cama.input” is prepared with those coordinates using R.

```
# Generating a sequence of grid-points for camaflood input data.,
grids.cama.input=data.frame(Lon=rep(seq(-180,179,by=1),times=180),Lat=rep(seq(90,-89,by=-1),each=360))
# use head(grids.cama.input,20) or tail (grids.cama.input,20) or summary(grids.cama.input) or dim(grids.cama.input) to get an idea about the dataframe.,

# Locating grids.cama.input coordinates falling within Canada.,
gps.canada=read.csv("C:/Research material _Ayushi Gaur/Ayushi Research work/Future runoff projection/jg_stationlist for CamaFlood model_input data points located within Canada.csv")
# use head(gps.canada,20) or tail (gps.canada,20) or summary(gps.canada) or dim(gps.canada) to get an idea about the dataframe.,
```

Figure 4.1. Locating grids of CaMa-Flood inputs coordinates lying within Canada.

4.3 Converting input runoff data from numerical to binary format.

The function provided in Appendix A (ii) does the conversion of numeric runoff data for one day to binary is the function “SUB.write.daily.bin”. Function “writeBIN” in R is used to do the conversion. Formatting of CaMa-Flood input runoff data in binary format is shown Figure 4.3.

Roff__20060101	2016-11-18 10:42 ...	Microsoft OneNot...	254 KB
Roff__20060102	2016-11-18 10:42 ...	Microsoft OneNot...	254 KB
Roff__20060103	2016-11-18 10:42 ...	Microsoft OneNot...	254 KB
Roff__20060104	2016-11-18 10:42 ...	Microsoft OneNot...	254 KB
Roff__20060105	2016-11-18 10:42 ...	Microsoft OneNot...	254 KB
Roff__20060106	2016-11-18 10:42 ...	Microsoft OneNot...	254 KB
Roff__20060107	2016-11-18 10:42 ...	Microsoft OneNot...	254 KB
Roff__20060108	2016-11-18 10:42 ...	Microsoft OneNot...	254 KB
Roff__20060109	2016-11-18 10:42 ...	Microsoft OneNot...	254 KB
Roff__20060110	2016-11-18 10:42 ...	Microsoft OneNot...	254 KB
Roff__20060111	2016-11-18 10:42 ...	Microsoft OneNot...	254 KB
Roff__20060112	2016-11-18 10:42 ...	Microsoft OneNot...	254 KB
Roff__20060113	2016-11-18 10:42 ...	Microsoft OneNot...	254 KB
Roff__20060114	2016-11-18 10:42 ...	Microsoft OneNot...	254 KB
Roff__20060115	2016-11-18 10:42 ...	Microsoft OneNot...	254 KB
Roff__20060116	2016-11-18 10:42 ...	Microsoft OneNot...	254 KB
Roff__20060117	2016-11-18 10:42 ...	Microsoft OneNot...	254 KB
Roff__20060118	2016-11-18 10:42 ...	Microsoft OneNot...	254 KB
Roff__20060119	2016-11-18 10:42 ...	Microsoft OneNot...	254 KB
Roff__20060120	2016-11-18 10:42 ...	Microsoft OneNot...	254 KB
Roff__20060121	2016-11-18 10:42 ...	Microsoft OneNot...	254 KB
Roff__20060122	2016-11-18 10:42 ...	Microsoft OneNot...	254 KB
Roff__20060123	2016-11-18 10:42 ...	Microsoft OneNot...	254 KB
Roff__20060124	2016-11-18 10:42 ...	Microsoft OneNot...	254 KB
Roff__20060125	2016-11-18 10:42 ...	Microsoft OneNot...	254 KB

Figure 4.2. Sample input runoff files for CaMa-Flood for the GCM for historical and future for each day.

4.4 After login the work directory under WinSCP, changes should be made by changing the data input, location, or if outputs needed, needs to be changed. Desirable outputs can also be fixed by making changes in this file.

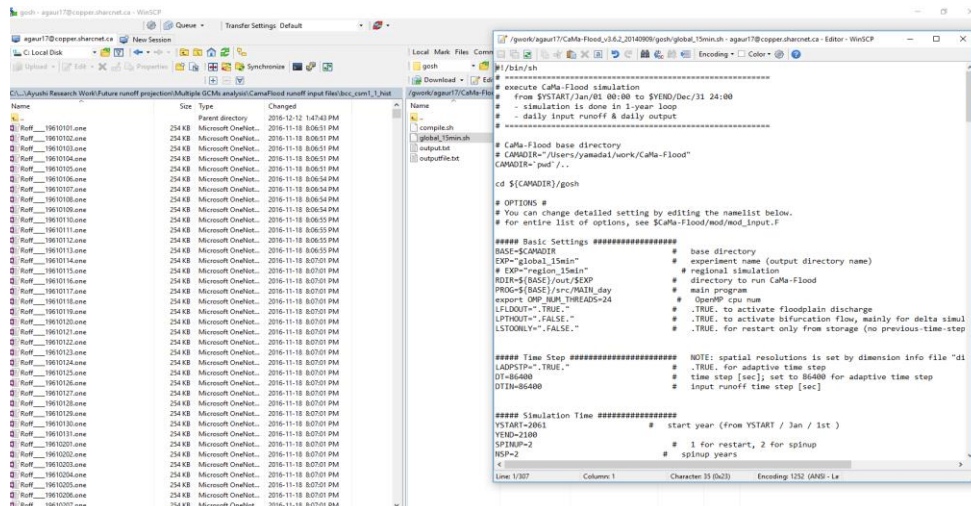


Figure 4.3. Editing in global_15min.sh file for getting the desirable timeline and output variables.

4.5. Modules and paths should be set in Mkinclude file before running the CaMa-Flood for runoff simulations (as shown in Figure 4.5). Changes in Mkinclude file is shown in Figure 3.3. Changes should be saved before running the model.

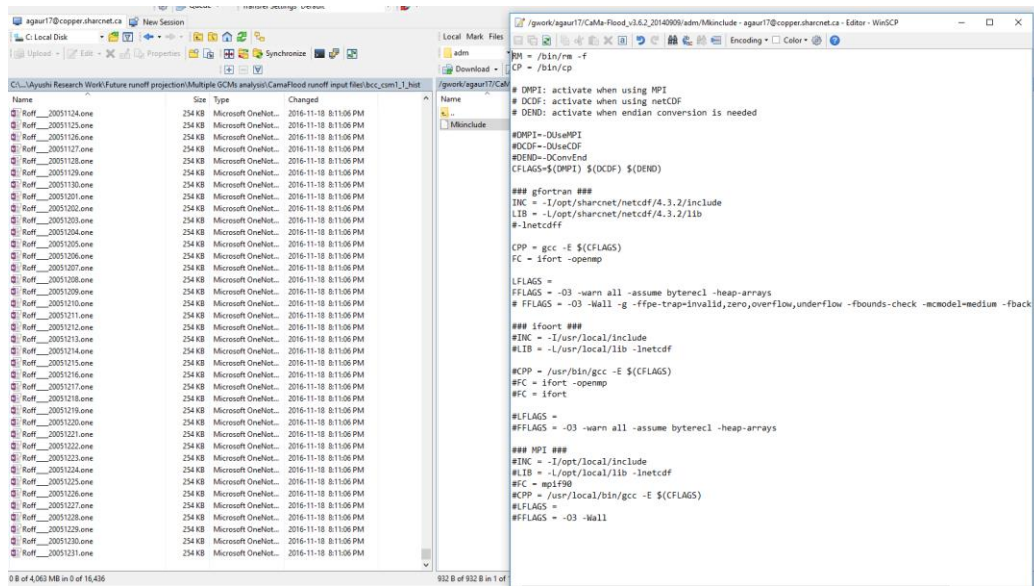


Figure 4.4. Edited Mkinclude file for CaMa-Flood model simulation.

4.6 Input runoff files should be transferred from the destination folder to the CaMa-Flood package through WinSCP (as shown in Figure 4.6).

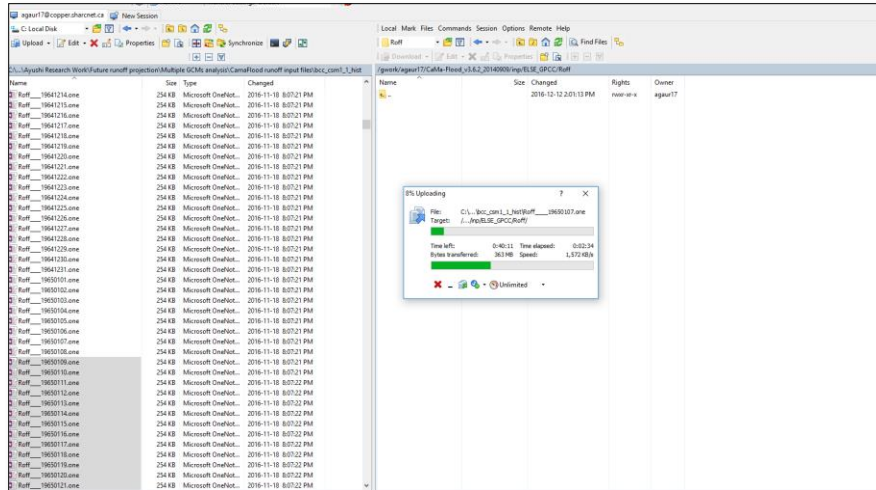


Figure 4.5. Transferring input files to the CaMa-Flood package in input folder.

4.7 CaMa-Flood software is run for the particular scenario using code shown in Figure 3.3.

Compilation and creation of executables is highlighted in Yellow as shown in Figure 4.7.

Command used to perform the model compilation and executable creation: “bash compile.sh yes”.

```

copper.sharcnet.ca - PuTTY
ifort -openmp day2mon.o -o day2mon -L/opt/sharcnet/netcdf/4.3.2/lib
ar -rv srcs.a calc_fldstg.o calc_rivout.o calc_fldout.o calc_pthout.o calc_damout.o calc_outpre.
.o calc_rivout_kine.o calc_stonxt.o calc_watbal.o create_outcdf.o create_outbin.o control_inp.o
control_phy.o control_out.o control_rest.o control_tstp.o init_inputnam.o init_map.o init_topo.o
init_cond.o init_time.o control0.o
r - calc_fldstg.o
r - calc_rivout.o
r - calc_fldout.o
r - calc_pthout.o
r - calc_damout.o
r - calc_outpre.o
r - calc_rivout_kine.o
r - calc_stonxt.o
r - calc_watbal.o
r - create_outcdf.o
r - create_outbin.o
r - control_inp.o
r - control_phy.o
r - control_out.o
r - control_rest.o
r - control_tstp.o
r - init_inputnam.o
r - init_map.o
r - init_topo.o
r - init_cond.o
r - init_time.o
r - control0.o
ifort -openmp -O3 -warn all -assume byterecl -heap-arrays MAIN_day.o srcs.a ../mod/mods.a ../l
ib/lib.a -o MAIN_day -L/opt/sharcnet/netcdf/4.3.2/lib
Compilation OK! Executable created: /work/agaur17/CaMa-Flood_v3.6.2_20140909/gosh/./src/MAIN_d
ay

```

Figure 4.6. Code compilation and creating executables.

4.8 CaMa-Flood model is run on PuTTY software and provided with a jobid and status (as shown in Figure 4.7).

```

copper.sharcnet.ca - PuTTY
ifort -openmp -O3 -warn all -assume byterecl -heap-arrays -I/opt/sharcnet/netcdf/4.3.2/include
day2mon.f90 -o day2mon.o
ifort -openmp day2mon.o -o day2mon -L/opt/sharcnet/netcdf/4.3.2/lib
ar -rv srcs.a calc_fldstg.o calc_rivout.o calc_fldout.o calc_pthout.o calc_damout.o calc_outpre.o
calc_rivout_kine.o calc_stomxt.o calc_watbal.o create_outcdf.o create_outbin.o control_inp.o
control_phy.o control_out.o control_rest.o control_tstp.o init_inputnam.o init_map.o init_topo.o
init_cond.o init_time.o control0.o
r - calc_fldstg.o
r - calc_rivout.o
r - calc_fldout.o
r - calc_pthout.o
r - calc_damout.o
r - calc_outpre.o
r - calc_rivout_kine.o
r - calc_stomxt.o
r - calc_watbal.o
r - create_outcdf.o
r - create_outbin.o
r - control_inp.o
r - control_phy.o
r - control_out.o
r - control_rest.o
r - control_tstp.o
r - init_inputnam.o
r - init_map.o
r - init_topo.o
r - init_cond.o
r - init_time.o
r - control0.o
ifort -openmp -O3 -warn all -assume byterecl -heap-arrays MAIN_day.o srcs.a ../mod/mods.a ../l
ib/libs.a -o MAIN_day -L/opt/sharcnet/netcdf/4.3.2/lib
Compilation OK! Executable created: /work/agaauri7/CaMa-Flood_v3.6.2_20140909/gosh/./src/MAIN_d
ay
-bash-4.1$ sqsub -q threaded -n 24 -r 4h --mpp=16g -o output.txt bash global_15min.sh
submitted as jobid 337887
-bash-4.1$ sqjobs
jobid queue state nopus nodes time command
-----
337887 threaded R 24 cop28 17s bash global_15min.sh
-bash-4.1$

```

Figure 4.7. Final code for running CaMa-Flood model simulation in PuTTY software.

4.9 A sample output file generated from CaMa-Flood is shown in Figure 4.9. Further, these output files can be accessed and analyzed using R statistical and programming language.

<input type="checkbox"/> fldare1961.bin	2017-04-20 12:42 ...	BIN File	1,478,250 KB	<input type="checkbox"/> fldare2061.bin	2017-04-18 3:15 PM	BIN File	1,478,250 KB
<input type="checkbox"/> fldare1962.bin	2017-04-20 12:48 ...	BIN File	1,478,250 KB	<input type="checkbox"/> fldare2062.bin	2017-04-18 3:19 PM	BIN File	1,478,250 KB
<input type="checkbox"/> fldare1963.bin	2017-04-20 12:53 ...	BIN File	1,478,250 KB	<input type="checkbox"/> fldare2063.bin	2017-04-18 3:23 PM	BIN File	1,478,250 KB
<input type="checkbox"/> fldare1964.bin	2017-04-20 12:59 ...	BIN File	1,482,300 KB	<input type="checkbox"/> fldare2064.bin	2017-04-18 3:28 PM	BIN File	1,482,300 KB
<input type="checkbox"/> fldare1965.bin	2017-04-20 1:04 AM	BIN File	1,478,250 KB	<input type="checkbox"/> fldare2065.bin	2017-04-18 3:32 PM	BIN File	1,478,250 KB
<input type="checkbox"/> fldare1966.bin	2017-04-20 1:09 AM	BIN File	1,478,250 KB	<input type="checkbox"/> fldare2066.bin	2017-04-18 3:36 PM	BIN File	1,478,250 KB
<input type="checkbox"/> fldare1967.bin	2017-04-20 1:14 AM	BIN File	1,478,250 KB	<input type="checkbox"/> fldare2067.bin	2017-04-18 3:41 PM	BIN File	1,478,250 KB
<input type="checkbox"/> fldare1968.bin	2017-04-20 1:19 AM	BIN File	1,482,300 KB	<input type="checkbox"/> fldare2068.bin	2017-04-18 3:45 PM	BIN File	1,482,300 KB
<input type="checkbox"/> fldare1969.bin	2017-04-20 1:24 AM	BIN File	1,478,250 KB	<input type="checkbox"/> fldare2069.bin	2017-04-18 3:49 PM	BIN File	1,478,250 KB
<input type="checkbox"/> fldare1970.bin	2017-04-20 1:29 AM	BIN File	1,478,250 KB	<input type="checkbox"/> fldare2070.bin	2017-04-18 3:54 PM	BIN File	1,478,250 KB
<input type="checkbox"/> fldare1971.bin	2017-04-20 1:33 AM	BIN File	1,478,250 KB	<input type="checkbox"/> fldare2071.bin	2017-04-18 3:58 PM	BIN File	1,478,250 KB
<input type="checkbox"/> fldare1972.bin	2017-04-20 1:38 AM	BIN File	1,482,300 KB	<input type="checkbox"/> fldare2072.bin	2017-04-18 4:03 PM	BIN File	1,482,300 KB
<input type="checkbox"/> fldare1973.bin	2017-04-20 1:43 AM	BIN File	1,478,250 KB	<input type="checkbox"/> fldare2073.bin	2017-04-18 4:07 PM	BIN File	1,478,250 KB
<input type="checkbox"/> fldare1974.bin	2017-04-20 1:48 AM	BIN File	1,478,250 KB	<input type="checkbox"/> fldare2074.bin	2017-04-18 4:12 PM	BIN File	1,478,250 KB
<input type="checkbox"/> fldare1975.bin	2017-04-20 1:52 AM	BIN File	1,478,250 KB	<input type="checkbox"/> fldare2075.bin	2017-04-18 4:16 PM	BIN File	1,478,250 KB
<input type="checkbox"/> fldare1976.bin	2017-04-20 1:57 AM	BIN File	1,482,300 KB	<input type="checkbox"/> fldare2076.bin	2017-04-18 4:20 PM	BIN File	1,482,300 KB
<input type="checkbox"/> fldare1977.bin	2017-04-20 2:01 AM	BIN File	1,478,250 KB	<input type="checkbox"/> fldare2077.bin	2017-04-18 4:25 PM	BIN File	1,478,250 KB
<input type="checkbox"/> fldare1978.bin	2017-04-20 2:05 AM	BIN File	1,478,250 KB	<input type="checkbox"/> fldare2078.bin	2017-04-18 4:29 PM	BIN File	1,478,250 KB
<input type="checkbox"/> fldare1979.bin	2017-04-20 2:10 AM	BIN File	1,478,250 KB	<input type="checkbox"/> fldare2079.bin	2017-04-18 4:33 PM	BIN File	1,478,250 KB
<input type="checkbox"/> fldare1980.bin	2017-04-20 2:14 AM	BIN File	1,482,300 KB	<input type="checkbox"/> fldare2080.bin	2017-04-18 4:38 PM	BIN File	1,482,300 KB
<input type="checkbox"/> fldare1981.bin	2017-04-20 2:19 AM	BIN File	1,478,250 KB	<input type="checkbox"/> fldare2081.bin	2017-04-18 4:42 PM	BIN File	1,478,250 KB
<input type="checkbox"/> fldare1982.bin	2017-04-20 2:23 AM	BIN File	1,478,250 KB	<input type="checkbox"/> fldare2082.bin	2017-04-18 4:47 PM	BIN File	1,478,250 KB
<input type="checkbox"/> fldare1983.bin	2017-04-20 2:28 AM	BIN File	1,478,250 KB	<input type="checkbox"/> fldare2083.bin	2017-04-18 4:51 PM	BIN File	1,478,250 KB
<input type="checkbox"/> fldare1984.bin	2017-04-20 2:32 AM	BIN File	1,482,300 KB	<input type="checkbox"/> fldare2084.bin	2017-04-18 4:55 PM	BIN File	1,482,300 KB
<input type="checkbox"/> fldare1985.bin	2017-04-20 2:37 AM	BIN File	1,478,250 KB	<input type="checkbox"/> fldare2085.bin	2017-04-18 5:00 PM	BIN File	1,478,250 KB
<input type="checkbox"/> fldare1986.bin	2017-04-20 2:42 AM	BIN File	1,478,250 KB	<input type="checkbox"/> fldare2086.bin	2017-04-18 5:04 PM	BIN File	1,478,250 KB
<input type="checkbox"/> fldare1987.bin	2017-04-20 2:46 AM	BIN File	1,478,250 KB	<input type="checkbox"/> fldare2087.bin	2017-04-18 5:09 PM	BIN File	1,478,250 KB
<input type="checkbox"/> fldare1988.bin	2017-04-20 2:50 AM	BIN File	1,482,300 KB	<input type="checkbox"/> fldare2088.bin	2017-04-18 5:13 PM	BIN File	1,482,300 KB
<input type="checkbox"/> fldare1989.bin	2017-04-20 2:55 AM	BIN File	1,478,250 KB	<input type="checkbox"/> fldare2089.bin	2017-04-18 5:18 PM	BIN File	1,478,250 KB
<input type="checkbox"/> fldare1990.bin	2017-04-20 2:59 AM	BIN File	1,478,250 KB	<input type="checkbox"/> fldare2090.bin	2017-04-18 5:22 PM	BIN File	1,478,250 KB

Figure 4.8. Output flood area files generated from CaMa-Flood.

4.10 Functions used to convert the output data from binary to numeric is provided in Appendix A (iii). Function “gridpoints.out1” has been used to find the indices from output files that are located within Canada and write the output data using “write.csv” for further output analysis.

5 Summary

Current global river routing models do not represent floodplain inundation dynamics realistically because the storage and movement of surface waters are regulated by small-scale topography rather than the commonly used spatial resolution of global models. In this study, we propose a new global river routing model, CaMa-Flood, which explicitly parameterizes the subgrid-scale topography of a floodplain, thus describing floodplain inundation dynamics. The relationship between water storage, water level, and flooded area in the model is decided on the basis of the subgrid-scale topographic parameters based on 1 km resolution digital elevation model. Global river routing model, CaMa-Flood, explicitly parameterizes the subgrid-scale topography of a floodplain, thus describing the floodplain inundation dynamics. The relationship between water storage, water level, and flooded area in the model is decided based on the subgrid-scale topographic parameters based on digital elevation model of the study region.

In this report, we also highlight the use of R programming language to read GCM runoff data, prepare inputs for running the model, and also analysing model outputs. Not solely is R programming free, but it's also open-source. The major advantage is, anyone can fix bugs and add features in R; also it allows to integrate with other languages like, C/C++, Java, Python, and enables to communicate with many data sources and other statistical packages.

Another major utility of this report is to provide the step-by-step guide as how the computational demanding large-scale simulations can be performed using a super computing facility, SHARCNET. SHARCNET is a consortium of 18 universities, colleges and research institutes providing a range of high performance computers and software, linked by an advanced fibre optics

network. Its overall aim is to promote the use of high-performance computing to accelerate the production of research results for researchers, Canadian industries, the economy and society in general. Large-scale, time-demanding simulations can be completed within the hours of time frame and thus make the research much faster and efficient.

6 References

- Arnell, N.W., 1999. Climate change and global water resources. *Global Environmental Change*, 9, S31-S49.
- Arnell, N.W., van Vuuren, D.P., Isaac M., (2011). The implications of climate policy for the impacts of climate change on global water resources. *Glob Environ Chang* 21:592–603.
- Arheimer, B., Lindström, G., (2015). Climate impact on floods – changes of high-flows in Sweden for the past and future (1911–2100). *Hydrol Earth Syst Sci* 19:771–784. doi:10.5194/hess-19-771-2015.
- Bates, P.D., De Roo, J.P.A., (2000). A simple raster-based model for flood inundation simulation. *Journal of Hydrology*, 236 (1–2), 54–77.
- Bates, P. D., M. S. Horrit, and T. J. Fewtrell (2010), A simple inertial formulation of the shallow water equations for efficient two-dimensional flood inundation modeling, *J. Hydrol.*, 387, 33-45, doi:10.1016/j.jhydrol.2010.03.027.
- Bell, V.A., Kay, A.L., Jones, R.G., Moore, R.J., Reynard, N.S., (2009). Use of soil data in a grid based hydrological model to estimate spatial variation in changing flood risk across UK. *Journal of Hydrology*, 377:335-350.
- Bell, V.A., Kay, A.L., Davies, H.N., Jones, R.G., (2016). An assessment of the possible impacts of climate change on snow and peak river flows across Britain. *Climatic Change*, doi:10.1007/s10584-016-1637-x.
- Bergström, S., (1995). The HBV model. In: Singh, V.P. (Ed.) *Computer Models of Watershed Hydrology. Water Resources Publications*, Highlands Ranch, CO., pp. 443-476.
- Bergström, S., (1976). Development and application of a conceptual runoff model for Scandinavian catchments, *SMHI Report RHO 7*, Norrköping, 134 pp.
- Beven, K. J., Kirkby, M. J., (1979). A physically based variable contributing area model of basin hydrology. *Hydrologic Science Bulletin*. 24(1):43-69.

- Biancamaria, S., Yamazaki, D., and Pedinotti, V., (2013), Impact of SWOT orbit subcycles on river studies, EGU 2013 General Assembly.
- Ciarapica, L., Todini, E., (2002). TOPKAPI: a model for the representation of the rainfall-runoff process at different scales. *Hydrological Processes*, 16, 207–229.
- Cohen, S., Kettner, A.J., and Syvitski, J.P.M., 2013. WBMsed: a distributed global-scale riverine sediment flux model - model description and validation. *Computers and Geosciences*, 53, 80-93, doi: 10.1016/j.cageo.2011.08.011.
- Collins, M., Booth, B.B.B., Harris, G.R., Murphy, G.M., Sexton, D.M.H., Webb, M.J., (2006). Towards quantifying uncertainty in transient climate change. *Climate Dynamics*, 27: 127-147.
- Dankers, R., and Feyen, L., (2008). Climate change impact on flood hazard in Europe: An assessment based on high resolution climate simulations, *J. Geophys. Res.*, 113, D19105, doi:10.1029/2007JD009719.
- Dankers, R., Feyen, L., (2009). Flood hazard in Europe in an ensemble of regional climate scenarios. *J. Geophys. Res. Atmos.* 114 doi:http://dx.doi.org/10.1029/2008jd011523.
- Döll, P., Lehner, B., Kaspar, F., (2002). Global modeling of groundwater recharge. In: Proc. Third Int. Conf. on *Water Resources and Environment Research* (ed. by G. H. Schmitz), vol. I, 322–326. Technical University, Dresden, Germany.
- Gosling, S.N., Bretherton, D., Haines, K., Arnell, W., et al. (2010) Global hydrology modelling and uncertainty: running multiple ensembles with a campus grid. *Philosophical Transactions of the Royal Society A – Mathematical Physical and Engineering Sciences* 368: 4005–4021.
- Gosling S, Arnell N et al. Simulating current global river runoff with a global hydrological model: model revisions, validation, and sensitivity analysis. *Hydrol. Process.*,25,1129-1145,2010.
- Gordon, C., C. Cooper, C.A. Senior, H.T. Banks, J.M. Gregory, T.C. Johns, J.F.B. Mitchell and R.A. Wood, 2000. The simulation of SST, sea ice extents and ocean heat transports in a version of the Hadley Centre coupled model without flux adjustments. *Clim. Dyn.*, 16, 147-168.

- Hirabayashi, Y., Mahendran, R., Koirala, S., Konoshima, L., Yamazaki, D., Watanabe, S., Kanae, S., (2013). Global flood risk under climate change, *Nature Climate Change*, 3(9), 816-821. doi:10.1038/nclimate 1911.
- Hirabayashi, Y., R. Mahendran, S. Koirala, L. Konoshima, D. Yamazaki, S. Watanabe, H. Kim, S. Kanae (2013) Global flood risk under climate change, *Nature Climate Change*, 3, 816-821, doi:10.1038/nclimate1911.
- Hunter, N. M., M. S. Horritt, P. D. Bates, W. D. Wilson, and M. G. F. Werner, (2005) An adaptive time step solution for raster-based storage cell modeling of floodplain inundation, *Advances in Water Resources*, 28, 975–991.
- Johns, T.C., Gregory, J.M., Ingram, W.J., Johnson, C.E., Jones, A., Lowe, J.A., Mitchell, J.F.B., Roberts, D.L., Sexton, D.M.H., Stevenson, D.S., Tett, S.F.B., Woodage, M.J., (2003). Anthropogenic climate change from 1860 to 2100 simulated with the HadCM3 model under updated emissions scenarios. *Climate Dynamics*, 20, 583–612.
- Lehner, B., Heiriches, P.D., Kaspar, F., (2006). Estimating the impact of global change on flood and drought risk in Europe: A continental, integrated analysis. *Climate change*, 75, 273-299.
- Lehner, B., Heiriches, P.D., Kaspar, F., (2006). Estimating the impact of global change on flood and drought risk in Europe: A continental, integrated analysis. *Climate change*, 75, 273-299
- Pappenberger, F., E. Dutra, F. Wetterhall, and H. L. Cloke (2012) Deriving global flood hazard maps of fluvial floods through a physical model cascade, *Hydrol. Earth Syst. Sci.*, 16, 4143-4156, doi:10.5194/hess-16-4143-2012.
- Roeckner, E., Brokopf, R., Esch, M., Giorgette, M., Hagemann, S., Kornbluh, L., (2006). Sensitivity of simulated climate to horizontal and vertical resolution in the ECHAM5 Atmosphere Model. *Journal of Climate*, 19, 3771–3791.
- Sorribas, M.V., Paiva, R.C.D., Melack, J.M., Bravo, J.M., Jones, C., Carvalho, L., Beighley, E., Forsberg, B., Costa, M.H., (2016). Projections of climate change effects on discharge and inundation in the Amazon basin. *Climatic Change*. <http://dx.doi.org/10.1007/s10584-016-1640-2>.

- Veijalainen, N., Lotsari, E., Alho, P., Vehviläinen, B., and Käyhkö, J., (2010). National scale assessment of climate change impacts on flooding in Finland. *J. Hydrol.*, 391, 333–350, 2010.
- Vormoor K., Lawrence, D., Heistermann, M., Bronstert, A., (2015). Climate change impacts on the seasonality and generation processes of floods — projections and uncertainties for catchments with mixed snowmelt/rainfall regimes. *Hydrol. Earth Syst. Sci.* 19: 913–931.
- Yamazaki, D., Lee, H., Alsdorf, E., Dutra, E., Kim, H., Kanae, S., Oki, T., (2012). Analysis of the water level dynamics simulated by a global river model: A case study in the Amazon River. *Wat. Resour. Res.* 48 (in the press, 2012).
- Yamazaki, D., G. A. M. de Almeida, and P. D. Bates (2013), Improving computational efficiency in global river models by implementing the local inertial flow equation and a vector-based river network map, *Water Resources Research*, published online.
- Yamazaki, D., T. Sato, S. Kanae, Y. Hirabayashi, and P. D. Bates (2014a), Regional flood dynamics in a bifurcating mega delta simulated in a global river model, *Geophys. Res. Lett.*, 41, doi:10.1002/2014GL059744.
- Yamazaki, D., H. Lee, D. E. Alsdorf, E. Dutra, H. Kim, S. Kanae, and T. Oki (2012a), Analysis of the water level dynamics simulated by a global river model: A case study in the Amazon River, *Water Resour. Res.*, 48, W09508, doi:10.1029/2012WR011869.
- Yamazaki, D., Kanae, S., Kim, H., Oki, T., (2011). A physically based description of floodplain inundation dynamics in a global river routing model. *Water Resour. Res.* 47, 1–21. doi:10.1029/2010WR009726.

7 Appendix A

- i. Function for interpolation using inverse distance method in R statistical and programming language.

```
Interpolate=function(ncfile,stationlist,date_ser)
{
  nc_file=nc_open(ncfile)
  #Opened file is used to extract longitude and latitude information:
  lon=ncvar_get(nc_file,"lon")
  lat=ncvar_get(nc_file,"lat")

  #Longitudes are adjusted to accommodate for a 0-360 scale in lon in NCEP data:
  if(max(lon)>180)
  lon[which(lon>180)]=lon[which(lon>180)]-360

  #Preparing the coordinate matrix:
  coord_mat=data.frame(Lon=rep(lon,length(lat)),Lat=rep(lat,each=length(lon)))

  #Performing nearest squared distance interpolation:
  d=do.call(cbind,lapply(1:nrow(stationlist), function(x) ((stationlist$Lon[x]-coord_mat$Lon)^2+(stationlist$Lat[x]-
coord_mat$Lat)^2)))
  close.ind=do.call(cbind,lapply(1:ncol(d), function(x) order(d[,x])[1:4]))
  w.close=do.call(cbind,lapply(1:ncol(close.ind), function(x) (1/d[close.ind[,x],x])/sum((1/d[close.ind[,x],x]))))

  #Find out which days should be extracted:
  #Extract the reference date info from the nc file.
  ref_date=as.Date(strsplit(strsplit(nc_file$dim[[which(names(nc_file$dim)
=="time")]]$units,"since")[[1]][2],"00:00:0.0")[[1]][1])
  if(grep("days",nc_file$dim[[which(names(nc_file$dim)=="time")]]$units)==1)
  {
    #If leap years are considered.
    data_dates=ref_date+ceiling(nc_file$dim[[which(names(nc_file$dim)=="time")]]$vals)

    #If leap years are not considered.
    if(ceiling(nc_file$dim$time$val[nc_file$dim$time$len])%%365==0)
    {
      all_dates=seq(from=ref_date,
                    to=as.Date(paste((year(ref_date)+ceiling(nc_file$dim[[which(names(nc_file$dim)
=="time")]]$vals[nc_file$dim$time$len]/365)),"-12-31",sep="")),
                    by="day")

      leap_dates=intersect(which(month(all_dates)==2),which(day(all_dates)==29))

      noleap_dates=all_dates
      if(length(leap_dates)>0)
      noleap_dates=all_dates[-leap_dates]

      data_dates=noleap_dates[ceiling(nc_file$dim[[which(names(nc_file$dim)
=="time")]]$vals[1]):ceiling(nc_file$dim[[which(names(nc_file$dim)=="time")]]$vals[nc_file$dim$time$len])]
    }
  }

  #If 360 days are considered in a year.
  if((ceiling(nc_file$dim$time$val[nc_file$dim$time$len])%%30==0) &&
ceiling(nc_file$dim$time$val[nc_file$dim$time$len])%%365!=0)
  {
```

```

year_ser=rep(year(ref_date):(year(ref_date)+ceiling(nc_file$dim[[which(names(nc_file$dim)
=="time")]]$vals[nc_file$dim$time$len]/360)),each=360)
month_ser=rep(rep(1:12,(length(year_ser)/360)),each=30)
day_ser=rep(1:30,(12*length(year_ser)/360))

all_dates=as.Date(sapply(1:length(year_ser), function(x) paste(year_ser[x],"-",month_ser[x],"-
",day_ser[x],sep="")))
all_dates=all_dates[which(all_dates==ref_date):length(all_dates)]
data_dates=all_dates[ceiling(nc_file$dim[[which(names(nc_file$dim)
=="time")]]$vals[1]):ceiling(nc_file$dim[[which(names(nc_file$dim) == "time")]]$vals[nc_file$dim$time$len])]
}

}

#Find out which time indices are to be extracted from the ncfile.
ind_dataext=which(as.character(data_dates) %in% as.character(date_ser))

if(length(ind_dataext)!=0)
{
#Extract dataset for extracted time and location indices:
#First extracting data at 4 nearest grids for each station and combining them as a list.
#In the output, each list component represents a station, columns within the list represent number of days and rows
represent the
#nearest neighbour datasets.
data_int=do.call(rbind,lapply(1:length(ind_dataext),
function(x) apply(matrix(ncvar_get(nc_file,varid=names(nc_file$var)[4], #Here assumed that
variable name of climate variable is at the end
start=c(1,1,ind_dataext[x]),

count=c(length(lon),length(lat),1))[matrix(close.ind)]*matrix(w.close,nrow=4,2,sum)))

write.csv(data.frame(date=data_dates[ind_dataext],data_int),
paste("C:/Research material _Ayushi Gaur/Ayushi Research Work/Future runoff projection/Multiple GCMs
analysis/Interpolated data-Canada/jg_",strsplit(strsplit(ncfile,"C:/Research material _Ayushi Gaur/Ayushi Research
Work/Future runoff projection/Multiple GCMs analysis/Inputs_hist_new/MRI-
ESM1/")[1][2],".nc")[1][1],".csv",sep=""))
}
}

```

- ii. Function for generating binary inputs for each day using R statistical and programming language.

#Write runoff data for a day in binary format needed for the camaflood model (Separate function)

```

SUB.write.daily.bin=function(runoff.day,date.day,scenario)
writeBin(object=runoff.day,endian="little",size=4,con=paste("C:/Research material _Ayushi Gaur/Ayushi Research
Work/Future runoff projection/Multiple GCMs analysis/CamaFlood runoff input
files/",scenario,"/Roff____",date.day,".one",sep=""))

```

- iii. Function used to analyze outputs.

```
library(rgdal)
```

```
flw.out.files=list.files("C:/Research material _Ayushi Gaur/Ayushi Research Work/Future runoff projection/Multiple
GCMs analysis/SHARCNET runs/Output _SHARCNET/MRI_ESM1_hist_r1",pattern="outflw.*.bin",full.names=T)
```

```
# Finding indices from output files that are located within Canada..
```

```
gridpoints.out=data.frame(lon=rep(seq(-180,179.75,by=0.25),times=720),lat=rep(seq(90,-89.75,by=-0.25),each=1440))
```

```

ind.out=Reduce(intersect,list(which(gridpoints.out$lon>-141),
                               which(gridpoints.out$lon<=-52),
                               which(gridpoints.out$lat>41),
                               which(gridpoints.out$lat<84)))

gridpoints.out1=gridpoints.out[ind.out,]

#Input canada shapefile:
can.shp <- readOGR("C:/Research material _Ayushi Gaur/Ayushi Research Work/NARR based validation of
CamaFlood/NARR runoff nc files/Results_NARR/CAN_adm_shp", "CAN_adm0")

if.inside.can=function(grid.point)
{
  #Projecting coordinates where satellite data is available:
  coordinates(grid.point) <- c("lon", "lat")
  #confirm that projection is same for both points and shapefile
  proj4string(grid.point) <- proj4string(can.shp)

  #Which satellite data points located within canada? stored in indices.can
  if.inside=is.na(over(grid.point, as(can.shp, "SpatialPolygons")))
  if(if.inside)
    as.numeric(names(if.inside))
}

indices.can2=row.names(gridpoints.out1)[-which(row.names(gridpoints.out1) %in% indices.can1$ind)]
write.csv(data.frame(ind=indices.can2,gridpoints.out[indices.can2,]),"C:/Research material _Ayushi Gaur/Ayushi
Research Work/Future runoff projection/jaishreeganeshg_stationlist for CamaFlood model output data points located
within Canada1.csv")

```

Appendix B: List of Previous Reports in the Series

ISSN: (Print) 1913-3200; (online) 1913-3219

[In addition to 78 previous reports \(No. 01 – No. 78\) prior to 2012](#)

Samiran Das and Slobodan P. Simonovic (2012). [Assessment of Uncertainty in Flood Flows under Climate Change](#). Water Resources Research Report no. 079, Facility for Intelligent Decision Support, Department of Civil and Environmental Engineering, London, Ontario, Canada, 67 pages. ISBN: (print) 978-0-7714-2960-6; (online) 978-0-7714-2961-3.

Rubaiya Sarwar, Sarah E. Irwin, Leanna King and Slobodan P. Simonovic (2012). [Assessment of Climatic Vulnerability in the Upper Thames River basin: Downscaling with SDSM](#). Water Resources Research Report no. 080, Facility for Intelligent Decision Support, Department of Civil and Environmental Engineering, London, Ontario, Canada, 65 pages. ISBN: (print) 978-0-7714-2962-0; (online) 978-0-7714-2963-7.

Sarah E. Irwin, Rubaiya Sarwar, Leanna King and Slobodan P. Simonovic (2012). [Assessment of Climatic Vulnerability in the Upper Thames River basin: Downscaling with LARS-WG](#). Water Resources Research Report no. 081, Facility for Intelligent Decision Support, Department of Civil and Environmental Engineering, London, Ontario, Canada, 80 pages. ISBN: (print) 978-0-7714-2964-4; (online) 978-0-7714-2965-1.

Samiran Das and Slobodan P. Simonovic (2012). [Guidelines for Flood Frequency Estimation under Climate Change](#). Water Resources Research Report no. 082, Facility for Intelligent Decision Support, Department of Civil and Environmental Engineering, London, Ontario, Canada, 44 pages. ISBN: (print) 978-0-7714-2973-6; (online) 978-0-7714-2974-3.

Angela Peck and Slobodan P. Simonovic (2013). [Coastal Cities at Risk \(CCaR\): Generic System Dynamics Simulation Models for Use with City Resilience Simulator](#). Water Resources Research Report no. 083, Facility for Intelligent Decision Support, Department of Civil and Environmental Engineering, London, Ontario, Canada, 55 pages. ISBN: (print) 978-0-7714-3024-4; (online) 978-0-7714-3025-1.

Roshan Srivastav and Slobodan P. Simonovic (2014). [Generic Framework for Computation of Spatial Dynamic Resilience](#). Water Resources Research Report no. 085, Facility for Intelligent Decision Support, Department of Civil and Environmental Engineering, London, Ontario, Canada, 81 pages. ISBN: (print) 978-0-7714-3067-1; (online) 978-0-7714-3068-8.

Angela Peck and Slobodan P. Simonovic (2014). [Coupling System Dynamics with Geographic Information Systems: CCaR Project Report](#). Water Resources Research Report no. 086, Facility for Intelligent Decision Support, Department of Civil and Environmental Engineering, London, Ontario, Canada, 60 pages. ISBN: (print) 978-0-7714-3069-5; (online) 978-0-7714-3070-1.

Sarah Irwin, Roshan Srivastav and Slobodan P. Simonovic (2014). [Instruction for Watershed Delineation in an ArcGIS Environment for Regionalization Studies](#). Water Resources Research Report no. 087, Facility for Intelligent Decision Support, Department of Civil and Environmental Engineering, London, Ontario, Canada, 45 pages. ISBN: (print) 978-0-7714-3071-8; (online) 978-0-7714-3072-5.

Andre Schardong, Roshan K. Srivastav and Slobodan P. Simonovic (2014). [Computerized Tool for the Development of Intensity-Duration-Frequency Curves under a Changing Climate: Users Manual v.1](#). Water Resources Research Report no. 088, Facility for Intelligent Decision Support, Department of Civil and Environmental Engineering, London, Ontario, Canada, 68 pages. ISBN: (print) 978-0-7714-3085-5; (online) 978-0-7714-3086-2.

Roshan K. Srivastav, Andre Schardong and Slobodan P. Simonovic (2014). [Computerized Tool for the Development of Intensity-Duration-Frequency Curves under a Changing Climate: Technical Manual v.1](#). Water Resources Research Report no. 089, Facility for Intelligent Decision Support, Department of Civil and Environmental Engineering, London, Ontario, Canada, 62 pages. ISBN: (print) 978-0-7714-3087-9; (online) 978-0-7714-3088-6.

Roshan K. Srivastav and Slobodan P. Simonovic (2014). [Simulation of Dynamic Resilience: A Railway Case Study](#). Water Resources Research Report no. 090, Facility for Intelligent Decision Support, Department of Civil and Environmental Engineering, London, Ontario, Canada, 91 pages. ISBN: (print) 978-0-7714-3089-3; (online) 978-0-7714-3090-9.

Nick Agam and Slobodan P. Simonovic (2015). [Development of Inundation Maps for the Vancouver Coastline Incorporating the Effects of Sea Level Rise and Extreme Events.](#) Water Resources Research Report no. 091, Facility for Intelligent Decision Support, Department of Civil and Environmental Engineering, London, Ontario, Canada, 107 pages. ISBN: (print) 978-0-7714-3092-3; (online) 978-0-7714-3094-7.

Sarah Irwin, Roshan K. Srivastav and Slobodan P. Simonovic (2015). [Instructions for Operating the Proposed Regionalization Tool "Cluster-FCM" Using Fuzzy C-Means Clustering and L-Moment Statistics.](#) Water Resources Research Report no. 092, Facility for Intelligent Decision Support, Department of Civil and Environmental Engineering, London, Ontario, Canada, 54 pages. ISBN: (print) 978-0-7714-3101-2; (online) 978-0-7714-3102-9.

Bogdan Pavlovic and Slobodan P. Simonovic (2016). [Automated Control Flaw Generation Procedure: Cheakamus Dam Case Study.](#) Water Resources Research Report no. 093, Facility for Intelligent Decision Support, Department of Civil and Environmental Engineering, London, Ontario, Canada, 78 pages. ISBN: (print) 978-0-7714-3113-5; (online) 978-0-7714-3114-2.

Sarah Irwin, Slobodan P. Simonovic and Niru Nirupama (2016). [Introduction to ResilSIM: A Decision Support Tool for Estimating Disaster Resilience to Hydro-Meteorological Events.](#) Water Resources Research Report no. 094, Facility for Intelligent Decision Support, Department of Civil and Environmental Engineering, London, Ontario, Canada, 66 pages. ISBN: (print) 978-0-7714-3115-9; (online) 978-0-7714-3116-6.

Tommy Kokas, Slobodan P. Simonovic (2016). [Flood Risk Management in Canadian Urban Environments: A Comprehensive Framework for Water Resources Modeling and Decision-Making.](#) Water Resources Research Report no. 095. Facility for Intelligent Decision Support, Department of Civil and Environmental Engineering, London, Ontario, Canada, 66 pages. ISBN: (print) 978-0-7714-3117-3; (online) 978-0-7714-3118-0.

Jingjing Kong and Slobodan P. Simonovic (2016). [Interdependent Infrastructure Network Resilience Model with Joint Restoration Strategy.](#) Water Resources Research Report no. 096, Facility for Intelligent

Decision Support, Department of Civil and Environmental Engineering, London, Ontario, Canada, 83 pages. ISBN: (print) 978-0-7714-3132-6; (online) 978-0-7714-3133-3.

Sohom Mandal, Patrick A. Breach and Slobodan P. Simonovic (2017). [Tools for Downscaling Climate Variables: A Technical Manual](#). Water Resources Research Report no. 097, Facility for Intelligent Decision Support, Department of Civil and Environmental Engineering, London, Ontario, Canada, 95 pages. ISBN: (print) 978-0-7714-3135-7; (online) 978-0-7714-3136-4.

R Arunkumar and Slobodan P. Simonovic (2017). [General Methodology for Developing a CFD Model for Studying Spillway Hydraulics using ANSYS Fluent](#). Water Resources Research Report no. 098, Facility for Intelligent Decision Support, Department of Civil and Environmental Engineering, London, Ontario, Canada, 39 pages. ISBN: (print) 978-0-7714-3148-7; (online) 978-0-7714-3149-4.

Andre Schardong, Slobodan P. Simonovic and Dan Sandink (2017). [Computerized Tool for the Development of Intensity-Duration-Frequency Curves Under a Changing Climate: Technical Manual v.2.1](#). Water Resources Research Report no. 099, Facility for Intelligent Decision Support, Department of Civil and Environmental Engineering, London, Ontario, Canada, 52 pages. ISBN: (print) 978-0-7714-3150-0; (online) 978-0-7714-3151-7.

Andre Schardong, Slobodan P. Simonovic and Dan Sandink (2017). [Computerized Tool for the Development of Intensity-Duration-Frequency Curves Under a Changing Climate: User's Manual v.2.1](#). Water Resources Research Report no. 100, Facility for Intelligent Decision Support, Department of Civil and Environmental Engineering, London, Ontario, Canada, 52 pages. ISBN: (print) 978-0-7714-3152-4; (online) 978-0-7714-3153-1.